G Model
PRE-6602; No. of Pages 5

ARTICLE IN PRESS

Precision Engineering xxx (2017) xxx–xxx

Contents lists available at ScienceDirect

Precision Engineering

journal homepage: www.elsevier.com/locate/precision

Development of a parameterized mechanical model of a chisel-edge grating ruling tool

Jirigalantu*, Xiaotian Li*, Xiaotao Mi, Kai Liu, Yuguo Tang

Changchun Institute of Optics, Fine Mechanics and Physics, Chinese Academy of Sciences, Changchun, 130033, China

ARTICLE INFO

Article history:
Received 21 August 2016
Received in revised form 1 March 2017
Accepted 16 June 2017
Available online xxx

Keywords:
Grating ruling tool
Parameterized model
Mechanical model
Chisel-edge tool

ABSTRACT

The parameterized mechanical model is proposed to optimize chisel-edge grating ruling tool parameters, eliminate corrugated grating lines, improve surfaces roughness of blaze plane, and reduce complex fabrication works such as step-by-step modification of tool guide angle. A mathematical model of force and torque between the diamond tool and the metallic film during the ruling process is deduced to realize optimized diamond tool geometrical parameter design. Then, grating ruling experiments are performed by tools with different guide angles of 75°, 95°, 115° and 135°, respectively. The experiments results agree well with the theoretical calculation value of force and torque. Experiments show that our proposed method is an effective way to solve the corrugated line and fluctuating problems on grating grooves, and can avoid complex and time-consuming technical operations such as step-by-step modification of tool guide angle. This illustrates the significance of our model for practical applications in the ruling of high-performance gratings.

1. Introduction

Diffraction gratings are regular arrays of lines, slits, grooves or variations of any optical property. They were first made in 1785 by Rittenhouse, but their scientific value was not fully appreciated until their reinvention by Fraunhofer in 1821 [1]. The ruling of a grating involves the extrusion and polishing of a metal coating on a grating substrate and the formation of stepped grooves after deformation [2], as shown in Fig. 1.

The quality of the extruded surface either side of a step affects the spectral orders, diffraction angles and diffraction efficiency of the grating. However, studies on the extruded forming of gratings have so far been mostly empirical in nature, and the theoretical study of the extruded forming of gratings is immature. For both academic knowledge and manufacturing, it is important to advance the systematic theoretical study of the extruding and polishing mechanism of the grating groove. The tool and film are the two primary objects in research on the extruding and polishing mechanism of the grating groove, and their interaction is the primary consideration in the study of the mechanism. Li [3], Li et al. [4] and Yang et al. [5] point out the importance of tool and film manufacturing technique respectively. Harrison [6], who performed researches on the ruling of large gratings and echelles using the MIT-C engine, observed that eight of the ruled large gratings failed because of the unclear mechanism between the ruling tool and the film, and only four large gratings were successfully ruled from a total of eighteen gratings.

The extruding and polishing of a grating film mainly involves plastic deformation associated with a small nonlinear elastic deformation, and the deformation mechanism is thus complex. The groove has a certain amount of resilience after the grating ruling tool passes, and the groove shape is mainly determined by the specific tool geometry in addition to the mechanical properties of the film. Harrison [7] stated that the greatest difficulties in producing the desired groove shape would probably arise from natural strains in, and plastic flow of, the material being cut, and storage in it of residual elastic energy. Verrill [8,9] analyzed the effects of tool alignment and tool wear on groove shape.

A universally used grating ruling tool is the chisel-edge (namely roof-edge or double-ended) tool [10]. The working region of this tool comprises one point (tool tip), two surfaces (tool side faces) and three edges (one main edge and two side edges) ground on natural diamond. In the ruling of a grating, as the tool moves forward across the film, the main edge of the tool incises off the film first, the side face of the tool then extrudes and polishes the film, and the side edge finally shapes the groove of the grating.

Generally, the cross section of a grating groove is asymmetric relative to a vertical line that passes through the point of the

* Corresponding authors.
E-mail addresses: jiri5998@163.com (Jirigalantu), lixt_1981@163.com (X. Li).

http://dx.doi.org/10.1016/j.precisioneng.2017.06.013

Please cite this article in press as: Jirigalantu, et al. Development of a parameterized mechanical model of a chisel-edge grating ruling tool. Precis Eng (2017), http://dx.doi.org/10.1016/j.precisioneng.2017.06.013

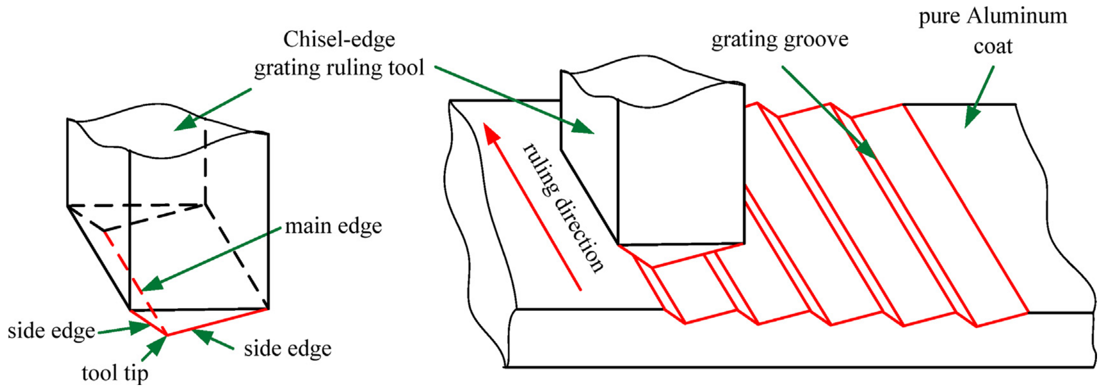

Fig. 1. Schematic view of a chisel-edge ruling tool and the grating ruling process.

groove bottom. An echelle grating with 79 grooves per millimeter, for example, might have a blaze angle of 63.4° and a non-blaze angle of approximately 27°, and correspondingly, the tool geometrical parameters must fit the technical requirements of ruling such a grating. The tool geometry not only determines the groove shape but also affects the quality of the grating. The development of a parameterized tool geometry model and mechanical model is meaningful to the study of the extruding and polishing mechanism of the grating groove.

2. Development of a parameterized mechanical model of diamond tool

The chisel-edge tool structure is presented in Fig. 2. The cross section has an asymmetrical "*V*" shape, and the main parameters are the tool orientation angle (*D*), non-orientation angle (*F*), and back obliquity angle (*H*). Fig. 2 presents the grating ruling direction, names of important parts of the tool and the geometrical relationship with the coordinate axes. Fig. 2 shows that the main edge of the tool lifts a little in the *X*–*Z* plane to form an angle with the *X*-axis, called the pitching angle (*E*). The two planes that form the pitching angle are called the orientation plane and non-orientation plane. The other two edges of the tool are formed by the intersections of the back oblique plane with the orientation plane and non-orientation plane and are thus called the orientation side edge and non-orientation side edge. The tool tip (*O*) is located at the Z-axis of the coordinate system, which is the intersection of the orientation plane, non-orientation plane and back obliquity plane. In developing the parameterized tool model, we see a cross section of the tool on the *X*–*Y* plane, as a triangle denoted $\triangle ABC$ in Fig. 2. The three internal angles of the triangle are α, β and λ, where λ is the sum of λ_1 and λ_2, and α is the guide angle of the tool. In the parameterized model of the tool, α is considered a variable while *D*, *F*, *H*, λ, *h* ($GO = h$), and *b* ($AC = b$) are constants, and it is set that $AB = c$, $BC = a$, $CO = e$, $CG = L$, $GP_3 = L_1$, $GP_4 = L_2$, h_a ($Gd_1 = h_a$), h_b ($Gd_2 = h_b$), as shown in Fig. 2.

The parameters have the relations

$$\sin(\lambda_1)\tan(D) = \sin(\lambda_2)\tan(F), \tag{1}$$

$$L = L_1 \ \tan(A_1)/\sin(\lambda_1)\tan(D), \tag{2}$$

$$L_1 = a\cos(\lambda_1) - h/\tan(E), \tag{3}$$

$$a/\sin(\alpha) = b/\sin(\beta) = c/\sin(\lambda). \tag{4}$$

Through above equations and the trigonometry of tool, we can calculate L, E, L_1, A_1, and β. The areas of the three planes of the tool denoted $S_{ABO} = S_H$, $S_{BCO} = S_d$ and $S_{AOC} = S_f$, on the basis of the areas of the planes and the projection areas of the planes on the *X*–*Y* plane, we obtain

$$\sqrt{p(p-a)(p-b)(p-c)}/h = a\ \cos(D)/(2\ \sin(D)) + b\ \cos(F)/(2\ \sin(F)) + c\ \cos(H)/(2\ \sin(H)), \tag{5}$$

where $p = (a + b + c)/2$.

Finally, through above equations and the trigonometry of tool, we calculate out parameter a. By similar way letting $Bp_3 = s_1$ and $Ap_4 = s_2$, we can calculate out parameters L_2, A_2, s_1, s_2, B_1, and B_2. Furthermore, based on the previous equations and parameters, we can develop a parameterized tool model.

When a chisel-edge tool extrudes and polishes a film, it experiences the resistance force of the film in the deformation process in the directions of the *X*, *Y*, and *Z* axes. We let pp_a denote the normal pressure on the orientation plane and $\mathrm{tt_a}$ denote the shear pressure on the orientation plane, as shown in Fig. 2. The included angles of the normal pressure pp_a and three coordinate axes are denoted x_a, y_a, and z_a. Similar to the case for the normal and shear pressures acting on the orientation plane, pp_b denotes the normal pressure acting on the non-orientation plane while tt_b denotes the shear pressure acting on the non-orientation plane. Tabor suggested that, for a Poisson's ratio of 0.3, the maximum contact pressure at the onset of plastic deformation can be related to the hardness of the softer material, H_n, in the form $pp = 0.6H_n$. Using Tresca's maximum shear stress criterion, we set $tt = H_n/5.65$ [11], and we can obtain the hardness H_n measured by nano-indenter. If the normal and shear pressures acting on each plane are *pp* and *tt*, then

$$pp_a = pp_b = pp = 0.6 \times H_n, \tag{6}$$

$$\mathrm{qq}_a = qq_b = tt = H_n/5.65. \tag{7}$$

Fig. 2 shows that $z_a = D$. We then obtain $\mathrm{x_a}$ from

$$\cos(x_a) = h\cos(D)/L. \tag{8}$$

and obtain y_a from

$$\cos^2(x_a) + \cos^2(y_a) + \cos^2(z_a) = 1. \tag{9}$$

Likewise, considering that $z_b = F$, we can obtain x_b and y_b. $\mathrm{S_{dx}}$, $\mathrm{S_{dy}}$ and $\mathrm{S_{dz}}$ denote the projections of $\mathrm{S_d}$ on the *Y*–*Z*, *X*–*Z* and *X*–*Y* planes respectively. Similarly, $\mathrm{S_{fx}}$, $\mathrm{S_{fy}}$ and $\mathrm{S_{fz}}$ denote the projections of $\mathrm{S_f}$ on the *Y*–*Z*, *X*–*Z* and *X*–*Y* planes respectively. The projection areas are $\mathrm{S_{dx}}$ is

$$S_{dx} = S_d \sin(x_a). \tag{10}$$

Likewise, the $\mathrm{S_{dy}}$, $\mathrm{S_{dz}}$, $\mathrm{S_{fx}}$, $\mathrm{S_{fy}}$, and $\mathrm{S_{fz}}$ are can be expressed as $\mathrm{S_{dx}}$, p_{xa} and p_{xb} denote the normal pressure distribution in the *X* direction, p_{ya} and p_{yb} denote the normal pressure distribution in the